Contamination-Free TEM for High-Resolution Imaging of Soft Materials

Shin Horiuchi[1] * and Takeshi Hanada[2]
[1]Nanosystem Research Institute, National Institute of Advanced Industrial Science and Technology (AIST), Tsukuba, Japan
[2]Consulting Zero Loss Imaging, Inc., Kawasaki, Japan
* s.horiuchi@aist.go.jp

Introduction

Element-selective imaging and analysis at atomic resolution have become possible by the recent advancements in TEM and STEM [1, 2]. However, the spatial resolution in images of soft materials can be limited by electron beam damage and/or contamination [3, 4]. This contamination is a carbonaceous layer deposited on the specimen surface as a result of electron bombardment. Beam-induced specimen contamination is caused by polymerization of hydrocarbons that are present in a TEM specimen chamber. The electron beam reacts with stray hydrocarbons in the beam's path to create hydrocarbon ions, which then condense and form carbon-rich polymerized film on the area being irradiated. Figure 1a shows contamination spots created on a carbon thin foil by illuminating a beam with an intensity of 5.6×10^4 el/nm·s at an accelerating voltage of 200 kV. The thickness of the contamination spots can be estimated by electron energy-loss spectroscopy (EELS). With increase in the irradiation period, the intensity of the zero-loss peak decreases, but the overall intensities in the energy-loss regions of the spectrum increase (Figure 1b). The thickness (D) can be estimated using the equation, $D = \Lambda \cdot ln(I_t/I_0)$, where Λ is the total mean free path for inelastic scattering, and I_t and I_0 are the integral intensities of the overall spectrum and the zero-loss peak, respectively. Using this equation, the thickness of the contamination was found to be about 600 nm with a 10-minute irradiation.

The sources of hydrocarbons are attributed to be vacuum pump oils, degradable or outgassing specimens, and poor vacuum practice. Even under ultra-high vacuum conditions, some contamination sources continue to reside inside the chamber and are not easily removed. Carbon is a predominant element in organic compounds. However, specimen contamination creates carbon-rich deposits on regions of interest in a specimen and disrupts specimen-oriented carbon analysis and imaging.

Reduction of Beam-Induced Specimen Contamination

We have developed an effective process for the cleaning of TEM chambers by using activated oxygen radicals [5]. Here a compact low-temperature plasma generator (Evactron 45, XEI Scientific, Inc., USA) was mounted on one of the accessory ports close to the specimen chamber as shown in Figure 2a. This device produces oxygen radicals from air that can chemically etch away contamination from the interior of a vacuum chamber [6]. Hydrocarbons and other organics are oxidized by the oxygen radicals from volatile oxides that can be easily pumped out from a TEM chamber. The plasma itself remains confined within the generator chamber, preventing ion bombardment damage to the microscope. Cleaning of an SEM has been successfully accomplished with this device, where the oxygen radicals were carried out of the plasma into the specimen chamber by convection flow and toward the roughing pump.

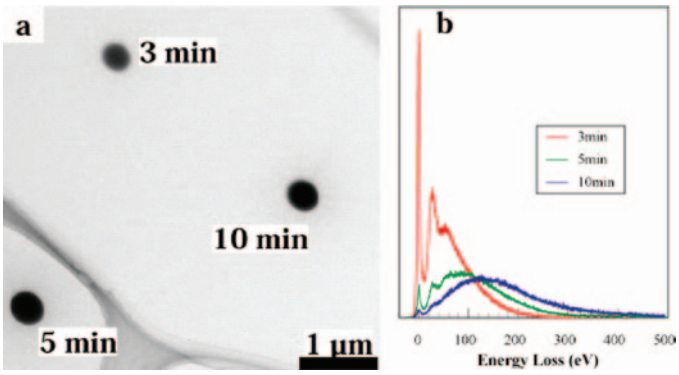

Figure 1: Beam-induced specimen contamination produced on a carbon thin foil by electron beam irradiation with an intensity of 5.6×10^4 el/nm·s. (a) TEM micrograph showing the contamination spots created by irradiation for 3, 5, and 10 minutes. (b) EELS spectra acquired from the contamination spots.

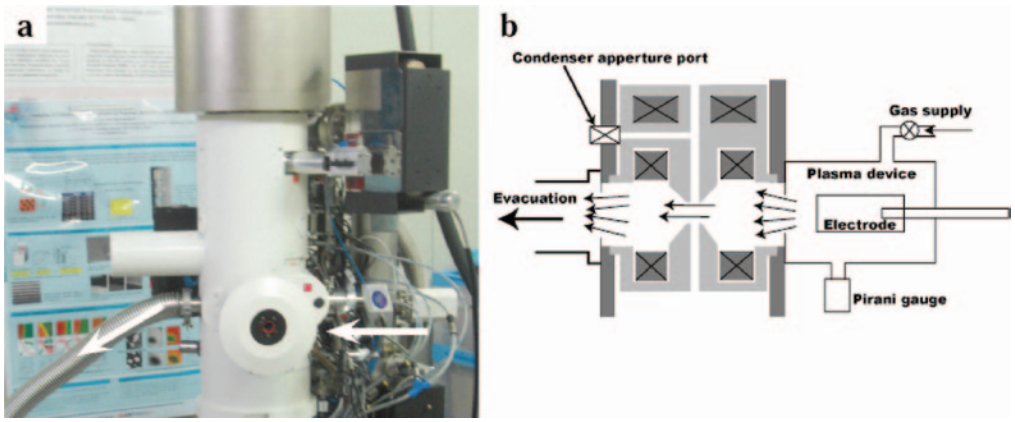

Figure 2: Cleaning of a TEM chamber using a compact plasma generator. (a) A photograph showing the plasma generator mounted on an accessory port close to the specimen chamber. The arrows indicate the flow direction of activated oxygen radical. (b) Schematic illustration showing the created flow of activated oxygen radials in the TEM.

 doi: 10.1017/S1551929510000313

AURIGA®

Information beyond Resolution

Unique Imaging | Precise Processing | Advanced Analytics | Future Assured

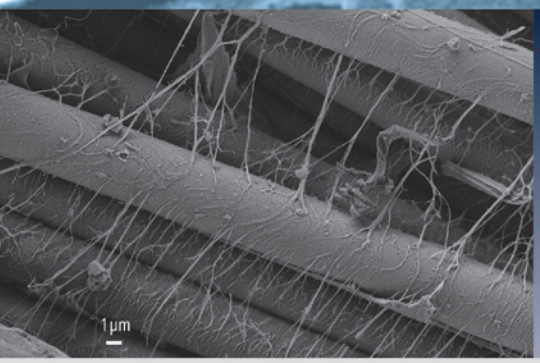

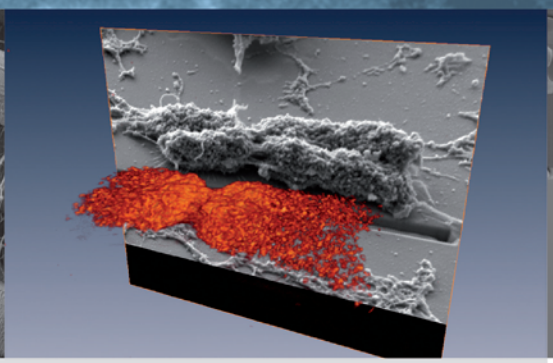

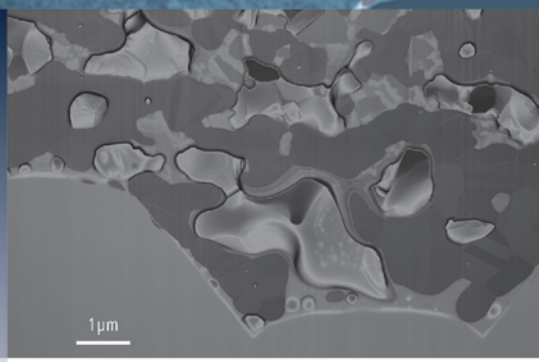

Carl Zeiss SMT Inc.

Enabling the Nano-Age World®

One Corporation Way
Peabody
MA 01960
USA

Tel. +1 978 / 826 7909
Fax +1 978 / 532 5696
info-usa@smt.zeiss.com
www.zeiss.com/nts

ZEISS

We make it visible.

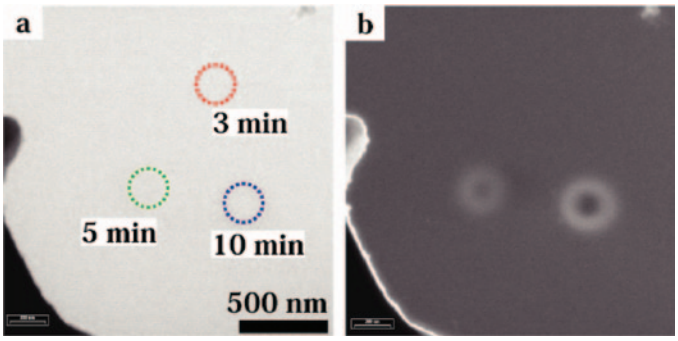

Figure 3: (a) Zero-loss and (b) energy-filtered image at 50 ± 10 eV, showing the contamination marks produced on an OsO_4 thin film after the cleaning.

However, beam-induced specimen contamination in the TEM cannot be reduced by simple operation of the plasma generator as was done for SEM. The reason is that the specimen chamber and the vacuum path of the TEM are considerably narrower, and not enough of the oxygen radicals can be supplied to the chamber by the evacuation with the roughing pump of the TEM. Therefore, we introduced an additional pumping system at the objective aperture port as illustrated in Figure 2b to create a viscous flow of oxygen radicals into the chamber. In this scheme, more oxygen radicals can travel through the specimen chamber where they can react with hydrocarbons in the chamber atmosphere and on chamber surfaces. Then, the specimen chamber was evacuated with an additional pump attached to the objective aperture port in which the pressure was kept at 0.4 torr by a controlled leak of air into the device. After the pressure stabilized, a high-frequency power (13.56 MHz) was applied to generate a plasma at 10 watts of power with room air as the feed gas. Gentle cleaning of the chamber was performed for 3 minutes, and then a nitrogen gas purge was used to flush the reacted products out of the chamber at 0.9 torr for 3 minutes. This cleaning/purging cycle was repeated 20 times.

After the cleaning, no contamination marks were seen on the specimen even after an electron beam bombardment was applied for 30 minutes without the use of an anticontamination device. Figure 3 shows contamination spots produced on an osmium tetraoxide (OsO_4) plasma-polymerized thin film. Because the contamination consists of carbon-rich products, the non-carbon supporting film could be observed with high contrast. The contamination spots were so thin that they could hardly be seen in the zero-loss image (Figure 3a); however, the contrast could be slightly enhanced in an energy-filtered image at the 50 ± 10 eV energy loss (Figure 3b). We have thus achieved the "contamination-free TEM" by gentle chemical cleaning of the specimen chamber with activated oxygen radicals.

High-Resolution Elemental Mapping of Carbon in Polymers

To examine the advantage of contamination-free TEM, we investigated the structure of a single polymer layer immobilized on the surface of a silica nanoparticle (SiNP). The sample used in this experiment is shown schematically in Figure 4. The synthesis procedure of this sample has been described in earlier publications [7]. The surface initiator, (2-bromo-2-methyl)propionyloxyhexyltriethoxysilane (BHE), was immobilized on the surface of the SiNP. Then, poly(2-methacryloyloxyethylphosphorylcholine) (PMPC) was grafted onto the BHE-immobilized SiNP by surface-initiated atom-transfer radical polymerization. The hydrodynamic radius of PMPC-immobilized SiNP (PMPC-SiNP) in water was estimated by dynamic light scattering to be 48.1 nm. The dimension of the PMPC polymer chains immobilized on SiNP is much larger than that of the corresponding free polymer, suggesting that the PMPC chains form "polymer brush" where the radially oriented chains stretch out perpendicularly from the silica surface. The PMPC-SiNP distributed on an OsO_4 thin film is shown in Figure 4, where only the SiNPs are visible.

Figure 5a and 5b are energy-filtered images of an isolated particle taken at the energy losses of 270 ± 10 eV and 315 ± 10 eV, respectively, which correspond to the pre- and

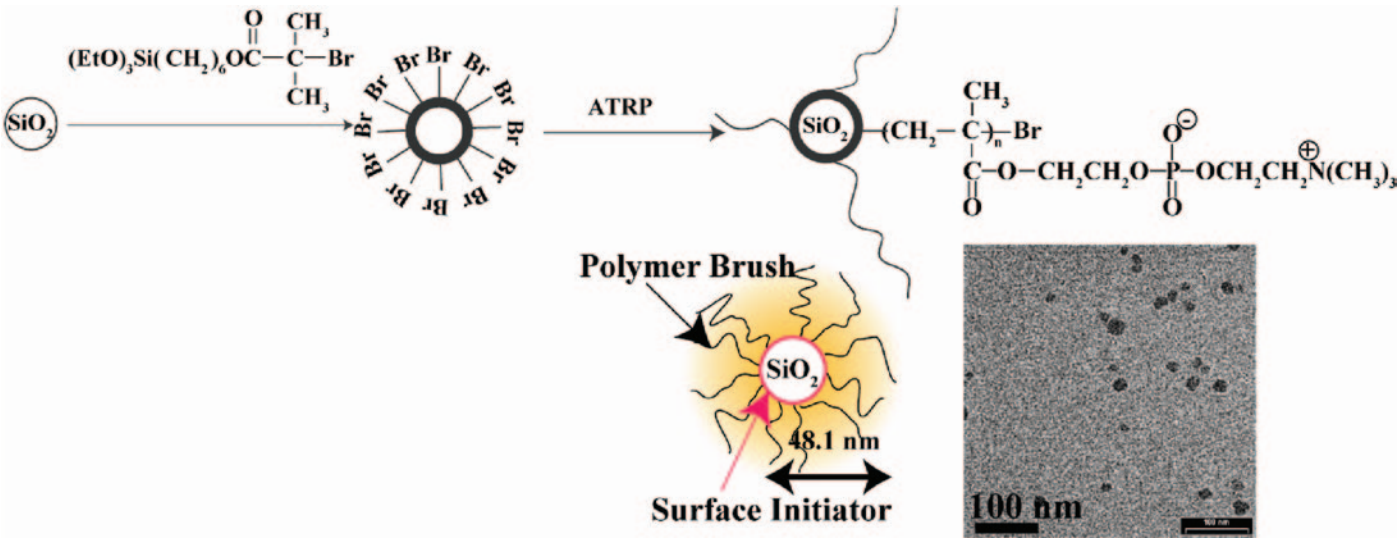

Figure 4: Schematic description of the synthesis of PMPC brushes on SiNP, illustration of PMPC-SiNPs brush structure, and Global TEM image showing the distribution of PMPC-SiNPs on an OsO_4 thin film.

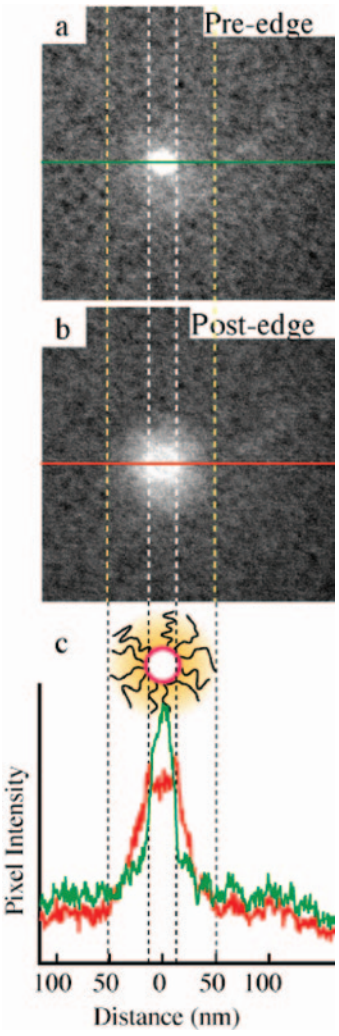

Figure 5: Pixel intensity profiles measured along the horizontal lines across the center of the PMPC-SiNP in (a) pre- and (b) post-edge images. Red and green lines in (c) correspond to the profiles obtained in (a) and (b), respectively. An illustration of the schematic structure showing the initiator and polymer brush parts is also shown in (c).

post-edge images for the carbon K-edge at 285 eV, respectively. The "contamination-free TEM" allows us to detect the polymer chains extending from the SiNP surface. The contrast difference between the two images indicates that the particle shown by the pre-edge image (Figure 5a) corresponds to the silica particle only, whereas the post-edge image (Figure 5b) shows the entire structure of the PMPC-SiNP. The gray-value intensity profiles along a horizontal line across the center of the SiNP were measured as shown in Figure 5c. The profile obtained from the pre-edge image (green line) indicates that the diameter of the SiNP is about 20 nm, whereas the diameter obtained from the post-edge image (red line) shows the PMPC brush thickness to be about 40 nm.

Figure 6 is another example of carbon elemental mapping showing the core-shell particle of silica-organic pigment hybrids in which the silica core is covered with phthalocyanine blue by dry mechanical milling [8]. This indicates the presence of the thin pigment layer surrounding the silica particle. The intensity profile obtained from the carbon map (Figure 6b) gives relatively sharp peaks as compared to the profile for the PMPC polymer brush (Figure 6a). The latter image indicates that the polymer chains are stretching from the surface of the core particle, whereas the former image of the low-molecular-weight pigment forms a dense thin layer on the surface of the silica particle.

Modifications of inorganic surfaces with organic compounds have been employed for improving dispersion, wetting, and adhesion. Thus, this analytical technique could be a promising approach for the development of various industrial materials. The detection of carbon in polymers is much simpler than detection of other light elements because of its high content. Thus, an image with high signal-to-noise

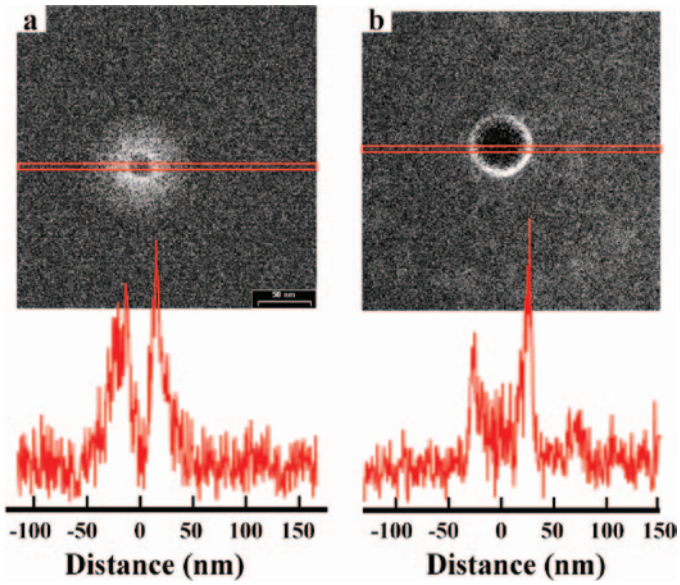

Figure 6: Carbon elemental maps of (a) PMPC polymer brush and (b) a phthalocyanine-silica hybrid particle. Intensity profiles are taken along the line shown in the corresponding images.

ratio can be obtained with lower electron doses than for other elements. Thus carbon analysis by EFTEM with high spatial resolution has the potential for improving soft-material nanoanalysis. Also, the contamination-free TEM will contribute to various analytical techniques requiring extended exposure time such as electron tomography, EELS, and nanobeam diffraction.

Conclusion

We have developed a cleaning process of a TEM by gentle chemical etching of the carbonaceous contaminations accumulated inside the specimen chamber. It can effectively reduce beam-induced specimen contamination, and this dramatically improves the quality of carbon elemental maps.

References

[1] K Kimoto et al., *Nature* 450 (2007) 702–704.
[2] D A Muller et al., *Science* 319 (2008) 1073–1076.
[3] L Reimer *Transmission Electron Microscopy*, Springer, Heidelberg, Berlin, Germany, 1997.
[4] A Kumao et al., *J Electron Microsc* 30 (**1981**) 161–170.
[5] S Horiuchi et al., *ACS Nano* 3 (2009) 1297–1304.
[6] R Vane and V Carlino, *Microsc Microanal* 11 (2005) 900–901.
[7] Y Matsuda et al., *Langmuir* 24 (2008) 8772–78.
[8] S. Horiuchi et al., *ACS Appl Mater Interface* 1 (2009) 977–981.

MT